

UCLA

Other Work

Title

Clean air in cities: Impact of the layout of buildings in urban areas on pedestrian exposure to ultrafine particles from traffic

Permalink

<https://escholarship.org/uc/item/6mg288qx>

Authors

Zhu, Liye
Ranasinghe, Dilhara
Chamecki, Marcelo
et al.

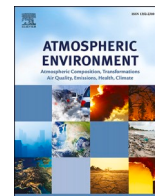
Publication Date

2021-05-01

DOI

10.1016/j.atmosenv.2021.118267

Peer reviewed



Clean air in cities: Impact of the layout of buildings in urban areas on pedestrian exposure to ultrafine particles from traffic

Liye Zhu^{d,a}, Dilhara Ranasinghe^{d,b}, Marcelo Chamecki^d, Michael J. Brown^c, Suzanne E. Paulson^{d,*}

^a School of Atmospheric Sciences, and Key Laboratory of Tropical Atmosphere-Ocean System (Sun Yat-sen University), Ministry of Education, and Southern Marine Science and Engineering Guangdong Laboratory, Zhuhai, 519082, China

^b Now at California Department of Pesticide Regulation, Sacramento, CA, 95812, USA

^c Los Alamos National Laboratory, Los Alamos, NM, 87545, USA

^d Department of Atmospheric and Oceanic Sciences, University of California, Los Angeles, CA, USA

HIGHLIGHTS

- Different built environments can change pollution levels by a factor of five.
- The QUIC model can reasonably reproduce UFP data for urban neighborhoods.
- Taller buildings and more ground level open space results in lower pollution.
- Pollution is highest for buildings in rows, lowest for buildings in a 'checkerboard'.
- Pollution levels drop off rapidly with height above the roadway.

ABSTRACT

Traffic-related pollutant concentrations are typically much higher in near-roadway microenvironments, and pedestrian and resident exposures to air pollutants can be substantially increased by the short periods of time spent on and near roadways. The design of the built environment plays a critical role in the dispersion of pollutants at street level; after normalizing for traffic, differences of a factor of ~ 5 have been observed between urban neighborhoods with different built environment characteristics. We examined the effects of different built environment designs on the concentrations of street-level ultrafine particles (UFP) at the scale of several blocks using the Quick Urban and Industrial Complex (QUIC) numerical modeling system. The model was capable of reasonably reproducing the complex ensemble mean 3D air flow patterns and pollutant concentrations in urban areas at fine spatial scale. We evaluated the effects of several built environment designs, changing building heights and spacing while holding total built environment volumes constant. We found that ground-level open space reduces street-level pollutant concentrations. Holding volume/surface area constant, tall buildings clustered together with larger open spaces between buildings resulted in substantially lower pollutant concentrations than buildings in rows. Buildings arranged on a 'checkerboard' grid with smaller contiguous open spaces, a configuration with some open space on one of the sides of the roadway at all locations, resulted in the lowest average concentrations for almost all wind directions. Rows usually prohibit mixing for perpendicular and oblique wind directions, even when there are large spaces between them, and clustered buildings have some areas where buildings border both sides of the roadways, inhibiting mixing. The model results suggest that pollutant concentrations drop off rapidly with height in the first 10 m or so above the roadways. In addition, the simulated vertical concentration profiles show a moderate elevated peak at the roof levels of the shorter buildings within the area. Model limitations and suggestions both for urban design are both discussed.

1. Introduction

As urbanization grows, the impact of traffic-related pollution on human health is an increasing concern. Traffic is a major source of primary air pollutants, including carbon monoxide (CO), carbon dioxide (CO₂), nitrogen oxides (NO_x), volatile organic compounds (VOCs), and

particulate matter (PM). Many studies have shown that living near busy roadways is associated with increased morbidity and mortality (Raaschou-Nielsen et al., 2013; Kheirbek et al., 2016), from respiratory and cardiovascular diseases (Lin et al., 2002; Riediker et al., 2004), birth and developmental effects (Becerra et al., 2013) and cancer (Pearson et al., 2000) among other diseases. PM from traffic is emitted as ultrafine

* Corresponding author.

E-mail address: paulson@atmos.ucla.edu (S.E. Paulson).

<https://doi.org/10.1016/j.atmosenv.2021.118267>

Received 22 July 2020; Received in revised form 27 December 2020; Accepted 9 February 2021

Available online 14 February 2021

1352-2310/© 2021 The Author(s).

Published by Elsevier Ltd.

This is an open access article under the CC BY-NC-ND license

(<http://creativecommons.org/licenses/by-nc-nd/4.0/>).

particles (UFP, particles smaller than 100 nm). Because UFP are short-lived due to high coagulation rates, they are quickly incorporated into larger particles (Choi and Paulson 2016) and they have relatively low urban background levels. UFP are highly elevated in fresh combustion sources, so they are an excellent tracer of fresh emissions from traffic. UFP may also be specifically responsible for differential health impacts associated with exposure to traffic emissions (Hoek et al., 2010; Chen et al., 2016; Heusinkveld et al., 2016; Manigrasso et al., 2017).

Because UFP concentrations are typically much higher in near-roadway microenvironments (Bowker et al., 2007; Morawska et al., 2008; Choi et al., 2012; Al-Dabbous and Kumar 2014), pedestrian and resident exposures can be strongly impacted by short periods of time spent on and near roadways (Lin et al., 2002; Behrentz et al., 2005; Manigrasso et al., 2017; Choi et al., 2018). In dense urban areas, near-roadway environments are not limited to sidewalks but can include most ground-level outdoor spaces. At the same time, UFP pollution levels in urban areas are highly variable (Patel et al., 2009; Choi et al., 2013). While our understanding of the built environment characteristics that influence street-level UFP concentrations is still developing, it is clear that the design of the built environment plays a major role (Boarnet et al., 2011; Boogaard et al., 2011; Buonanno et al., 2011; Pirjola et al., 2012; Choi et al., 2016; Ranasinghe et al., 2018).

Here we consider the effects of a set of six idealized building configurations on the concentrations of traffic-related or other pollution and resulting pedestrian exposures using a modeling framework. The Quick Urban and Industrial Complex (QUIC) transport and dispersion model (Brown 2018) was used to simulate the complex air flows and pollutant dispersion. As a first step, we evaluated the QUIC model's ability to reproduce measured data using the extensive field dataset from the Los Angeles (LA) area reported by Choi et al. (2016). The Choi et al. (2016) study was designed to examine the effects of the built environment, traffic patterns, and micrometeorology on street-level UFP concentrations at the scale of a few city blocks. We then explored the impact of open space interspersed with tall buildings on pollutant concentrations at street level, as well as the effects of clustering buildings, spacing them evenly or arranging them in rows in dense urban areas. We also explored the potential of using the QUIC model to better understand the vertical distribution of pollution in different built environments with a set of choices about urban building configurations and interpret the results within the context of urban planning, including recommendations for future urban design.

2. Methodology

2.1. QUIC model background

The Quick Urban & Industrial Complex (QUIC) model is a fast-response dispersion modeling system. It consists of two different wind solvers, the QUIC-URB empirical-diagnostic urban wind model (Gowardhan et al., 2011) and the QUIC-CFD computational fluid dynamics wind solver (Röckle 1990), the QUIC-PLUME "urbanized" Lagrangian random-walk dispersion model, and the QUIC-GUI graphical user interface. QUIC-URB was developed to rapidly calculate 3-D wind fields in cities using a suite of empirical parameterizations and mass conservation. It was based on work described in Röckle's thesis (Röckle 1990) and was later improved with modifications to empirical schemes so that it could be applied to urban environments (Brown 2018). QUIC-PLUME is a Lagrangian random-walk dispersion model that has been adapted to account for local and non-local building-induced turbulence. QUIC-GUI allows the user to import building layouts, define wind speeds and directions, choose pollutants, types of release, and release locations, and visualize mean wind flow and plume dispersion patterns. The QUIC modeling system has been extensively evaluated against full-scale tracer field experiments and reduced-scale wind-tunnel experiments (Brown 2018).

2.2. Model configurations

The building information for the 2.5×2.5 city-block size modeling domains (or larger if the measurement data used to validate the model covered a slightly larger area) was extracted from the Los Angeles Region Imagery Acquisition Consortium (LARIAC2) Geographic Information System (GIS) data (LARIAC 2009). The QUIC model imports buildings, vegetative canopies and point trees, however tree canopies were not included here because the input data were not available in the GIS data. Since the LARIAC2 database does not identify parking structures as buildings and they are required to accurately model the built environment, we added parking structures manually to our built environments when necessary.

We used meteorological data, including wind speed and wind direction from the measurements described in Choi et al. (2016) for each site and date, together with the calculated Monin-Obukhov length (Seinfeld and Pandis 1998). The meteorological measurements were made with sonic anemometers placed at street level, on roof tops or in a nearby park on each measurement day. We used rooftop wind measurements as initial winds to drive QUIC, and then evaluated the capability of QUIC by comparing simulated wind fields to observed wind measurements at street level. For the sites for which we did not have measurements on a roof or in a nearby park, we used the nearest available weather station. Details and calculations with the input meteorological data and corresponding weather stations are described in the supplementary material (Table S1). The wind fields from the QUIC-URB model were used to simulate the pollution dispersion and pollution concentrations in QUIC-PLUME model. QUIC is a fast response model: a sixteen million grid cell problem took ~ 50 s to run on a Core i5-7200u processor with 8 GB ram Dell laptop, for example.

As our measurement data covers $\sim 2 \times 2$ city blocks, we select 2.5×2.5 city blocks as our simulation domain (Fig. 1) or a correspondingly larger area for the rectangular areas. The model parameters were specified as follows. The height of the simulation domain was about 20 m above the highest building (250 m for site 1; 200 m for sites 2–4; 30 m for site 5) and the horizontal resolution was $5 \text{ m} \times 5 \text{ m}$. The vertical grid cell size was 0.4 m for the first 10 simulation grid levels; this was increased parabolically to the top of the domain. The traffic pollution tracer was released at the second level above the ground (0.4–0.8 m), corresponding to the height of most tailpipes. The pollution tracer was defined as a continuous line source placed along the main and sub-main streets in 2×2 city blocks (red lines in Fig. 1 left panel). Because accurate determination of UFP emission rates for the mixed fleets at each location is not possible, and simulating individual particles is computationally expensive, we did not simulate UFP per vehicle in the model. Instead, we set line sources at both main streets and sub-main streets that continuously release particles at constant rate. The calculated UFP concentrations on the streets were averaged for each morning ('am') or afternoon ('pm') session for each day and site and compared to measured concentrations that had been normalized by observed traffic flows (Choi et al., 2016). Thus, the choice of a constant source strength for every site to compare to traffic-normalized field data does not affect the comparison between the simulated and observed results.

The modeled arbitrary particle concentrations were adjusted to compare to the observations by assuming the model results and observations should have a slope of unity and intercept of zero (see Fig. 2). The original model output was plotted against the observational data and the intercept and slope of the resulting linear regression were used to adjust the model results to give the results shown in Fig. 2. Since this process only linearly adjusts the magnitude of simulated concentrations, the relative differences among built environments still remain. To match the observations collected with a mobile platform driving on the streets (yellow bands in Fig. 1), the average UFP concentration for each site and session was calculated by averaging the concentrations 0.4–2 m above ground level (AGL) in the model over all street grids within the domains. Fig. 1 shows the Broadway & 7th site with the building shapes in the



Fig. 1. Building shapes and the QUIC simulation domain in 2D and 3D Google Earth views for the Broadway & 7th site. The yellow bands in QUIC map are the main and sub-main streets and indicate the driving pattern where measurements were collected. Red lines are the line sources from the traffic. Light yellow squares in Google Earth satellite view are the 2×2 blocks we are focusing on. The colors of the buildings from dark blue to red represent the building height from low to high. (For interpretation of the references to color in this figure legend, the reader is referred to the Web version of this article.)

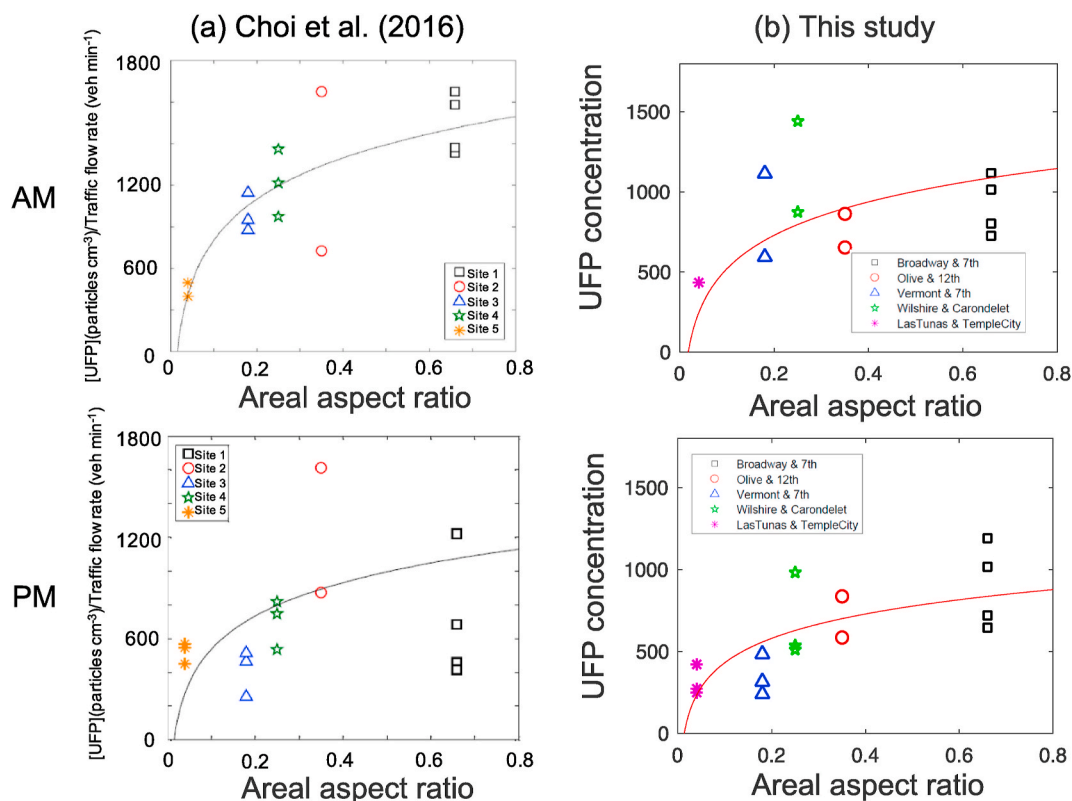


Fig. 2. The relationship between area aspect ratio ($A_{r,area}$) and UFP adjusted concentration for each site and measurement day from (a) mobile observations of Choi et al. (2016) and (b) the QUIC area-averaged simulations. The definitions of markers and colors match those in Fig. 2. The red lines in the right column plots are the log-fit lines in order to be consistent with the analysis method in Choi et al. (2016). (For interpretation of the references to color in this figure legend, the reader is referred to the Web version of this article.)

QUIC model and the Google Earth satellite map. The building shapes and simulation domains for the remaining four sites are shown in the supplementary material (Figure S1).

2.3. Observational data and areal aspect ratio parameter

The observational data in the Choi et al. (2016) study was collected in five areas with distinct building configurations that are common in

the Los Angeles area. They were collected with a mobile platform that was driven on the sampling route 25–40 times during each ~2-h morning or afternoon sampling session on 3–4 days at each site. Measurement data were GPS corrected, binned and averaged (Ranasinghe et al., 2016). The block-scale UFP concentrations had a strong direct relationship with the vertical turbulence intensity in the afternoons and the areal aspect ratio ($A_{r,area}$, described next) in the mornings (Choi et al., 2016). The vertical turbulence intensity is influenced by the built

environment, so while the built environment has a more direct impact on morning pollutant concentrations, it also appears to influence afternoon concentrations. In this dataset, morning wind speeds were low, averaging at about 0.98 m s^{-1} , and the afternoons were higher, averaging at 1.73 m s^{-1} . Presumably different heating of sides of buildings and other surfaces were also more significant in the afternoons.

The Areal Aspect Ratio (Ar_{area} , unitless) developed by Choi et al. (2016) is calculated based on the building area-weighted building height (H_{area} , m), the amount of open space (A_{open} , m^2), the area of the site (A_{site} , m^2), and the diagonal block length (L_{diag} , m) (Choi et al., 2016):

$$Ar_{area} = \frac{H_{area}}{L_{diag} \times (A_{open}/A_{site})} \quad (1)$$

This relationship was chosen from a set of metrics that combined building heights and footprints, density and open space as it provided the best fit of the observations. We tried to reproduce the same relationship between the UFP concentrations and building Ar_{area} with the QUIC model simulation using measured meteorological data, including wind speed and direction to drive the QUIC model.

3. QUIC model evaluation

Before we explored the various built environment configurations with the QUIC model, we evaluated the ability of the model to successfully simulate the observational dataset (Choi et al., 2016) collected at five sites with distinct building configurations found in the Los Angeles area. The five distinct building configurations include all low buildings (Las Tunas and Temple City), a tall street canyon (Broadway and 7th), a site with a wall of medium-tall buildings on one side of the main road adjacent to a park (Wilshire and Carondelet), and sites with one (Olive and 12th) and two isolated skyscrapers (Vermont and 7th), respectively, surrounded by 1–3 story buildings and open space.

Fig. 2 shows the average UFP concentrations for measurements (left panels) and model simulations (right panels) for each site and measurement session plotted against corresponding Ar_{area} for mornings and afternoons to compare with the analysis of the observational data as in Choi et al. (2016). Each point indicates the average for an individual ~ 2 -h measurement session; multiple points of the same color/shape were collected on different days at the same site. As Choi et al. (2016) found the best fit line to be of the form $y = a \times \log(Ar_{area}) + b$, we use this expression to fit our simulation results as well. Both the modeled and observed UFP concentrations exhibit strong relationships between with Ar_{area} ; the log best-fit curves (red lines) for the model have $r = 0.50$, am, $r = 0.72$, pm, respectively. UFP concentrations increasing sharply with Ar_{area} at low Ar_{area} (<0.2) and more slowly at higher Ar_{area} . The measurement data indicates that after normalizing for traffic, the built environment has a large impact on measured pollutant concentrations; the highest measured values, observed in the area with street canyons were 5–6 times the lowest values which were observed in a neighborhood with single story buildings. The simulations capture a similar range (Figs. 2 and 3).

Fig. 3 shows the UFP concentrations from QUIC simulations and observations plotted against each other. The 1:1 linear regression line (red line) has reasonably high r values of 0.58 and 0.50 for the mornings and afternoons respectively. The green dashed lines represent the \pm root mean square error (RMSE) interval, and red dotted lines represent the 90% confidence level that the prediction interval for which the next observational point will fall within the band (only the upper confidence intervals appear at this scale; the lower lines fall below the frame). All of the values are within the 90% confidence band (red) and most of them are within the RMSE interval (green).

Taken together, the results show the model does an acceptable job of reproducing the impact of the built environment on pollutant concentrations. There are several potential reasons for the scatter. These

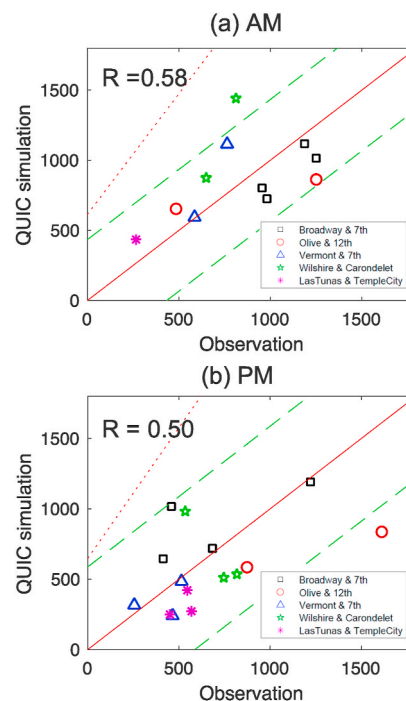


Fig. 3. Comparisons of UFP concentrations from QUIC simulations with observations from Choi et al. (2016). The red lines indicate both the linear regression line and the 1:1 line. Each point indicates the average concentration measured in a ~ 4 block area over the span of ~ 2 h during which windspeeds, directions and atmospheric structure were reasonably stable Choi et al. (2016); each one was measured on a different day. The R value is 0.58 in the morning case and 0.50 in the afternoon, respectively. The green dashed lines represent \pm root mean square error (RMSE). The red dotted lines represent 90% confidence level that the prediction of next observational point will fall within the band. (For interpretation of the references to color in this figure legend, the reader is referred to the Web version of this article.)

include differences in emissions between sites and sessions arising from variations in the vehicle fleets; sites had different average fleet ages and proportions of heavy-duty vehicles. Even for the same site, as small numbers of high emitting vehicles can overwhelm large numbers of cleaner vehicles (Choi et al., 2013), traffic-normalized emissions may have varied between sessions. Model-related reasons include the lack of vegetation and traffic-induced turbulence in the model. Model related limitations are discussed more in section 4.3.

4. Idealized built environment simulations

In the previous section, we were able to reasonably reproduce the relationship between street-level UFP concentrations and the built environment parameter Ar_{area} at five sites in Southern California. The observational sites were very different from one another and span a large portion of variability in configurations and values of Ar_{area} in urban areas worldwide. More uniform built environments that can be more common both in much older cities and in newer planned areas of developing cities. Here we explore six more regular building configurations that could be design choices for modern urban planners. We also examined the vertical distributions of UFP in our simulations to inform potential exposures of residents living on higher floors.

4.1. Effects of six built environment configurations on UFP concentrations at street level

We designed six idealized built environments (Types 1–6) with identical building volumes of 15.3 m^3 building volume/ m^2 ground area (Fig. 4). The total volume of real city blocks varies widely; the

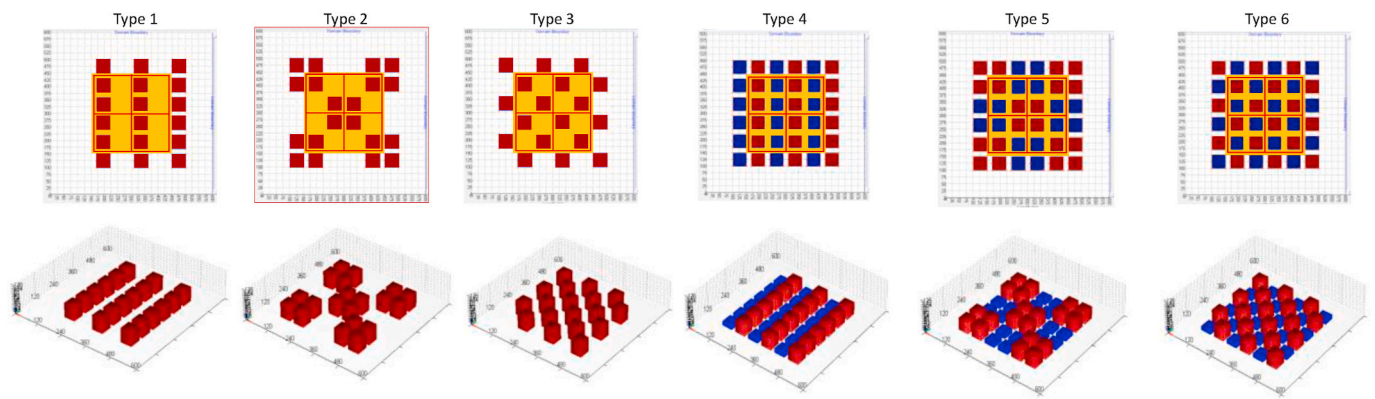


Fig. 4. Six model-built environment configurations. The main, sub-main streets and the open space between buildings within the 2×2 blocks are highlighted with yellow. The upper row shows the 2D visualization, and the lower row shows the 3D visualization. Buildings are shown in red or blue; open space is white. Red lines are the line sources from the traffic. The height of all buildings of Type 1–3 is 60 m. For Type 4–6, the height of blue buildings is 15 m, and the height of red buildings is 45 m. (For interpretation of the references to color in this figure legend, the reader is referred to the Web version of this article.)

neighborhoods included in the observational dataset had 42, 8.8, 3.6, 8.3 and $1.5 \text{ m}^3/\text{m}^2$ building volume of a city block for Broadway & 7th, Olive & 12th, Vermont & 7th, Wilshire & Carondelet and Temple City & Las Tunas respectively (Choi et al. (2016)). Building heights also varied widely; in the observational data the maximum building height ranged from 8 to 130 m; two of the sites had maximum heights of 57–58 m, corresponding to 15–20 story buildings. Similar to these, we used a maximum building height of 60 m, and a footprint of a reasonably representative tall building of 50×50 m, for building layout types 1–3. To hold the built environment volumes and building footprints constant and change the amount of open space, we cut the taller buildings to 45 m and added the extra volume as 15 m buildings for layout types 4–6. Streets were set to be 20 m wide, including sidewalks. This is at the lower end of the street widths in the observational data from Los Angeles in Choi et al. (2016), but Los Angeles has particularly wide streets, so we chose a value closer to the lower end to be more generally representative.

As for the simulations above, we released source particles along every main and sub-main street in the 2×2 city block domains and scaled the results by the source strength as described in section 2.2. However, unlike the simulations in the Los Angeles cases, we included not only the streets but also the open spaces between buildings when we averaged the street level concentrations over the area (see yellow area in Fig. 4). This is because here we focused on potential for human exposure and thus put more emphasis on diagonal walkways, playground and other uses of open space and somewhat less on the sidewalks adjacent to the roadways and in the roadway itself.

Ground level UFP concentrations were strongly impacted by the wind direction. While important factor for the measured data, its impact was more extreme for the modeled built environments because of their regularity. Thus, for each type of built environment, we simulated UFP concentrations using several wind directions (Fig. 5). In Fig. 5, we show the average UFP concentrations over all open space within the yellow area (see Figs. 4 and 6) at street level (0.4–2 m AGL). For these simulations, the background wind speed was fixed at 1 m s^{-1} at 20 m above ground level (AGL) for all simulations. This relatively low wind speed was commonly observed in urban areas, and lower wind speeds were associated with higher pollutant concentrations and thus represented times of day that were of greater concern (Choi et al., 2012; Ranasinghe et al., 2018). A similar comparison with averages over only the main and sub-main streets within the yellow area is shown in SI Fig. S3. The same general pattern was observed, but the differences between types were much smaller, because the particles were released on the streets, so the particle concentrations were more impacted by direct emissions and less by dispersion.

The UFP concentrations were strongly dependent on wind direction

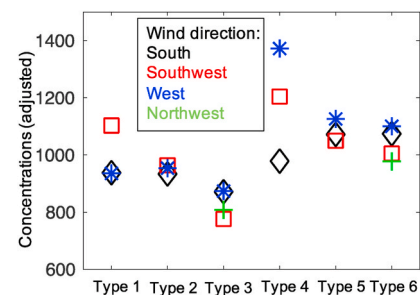
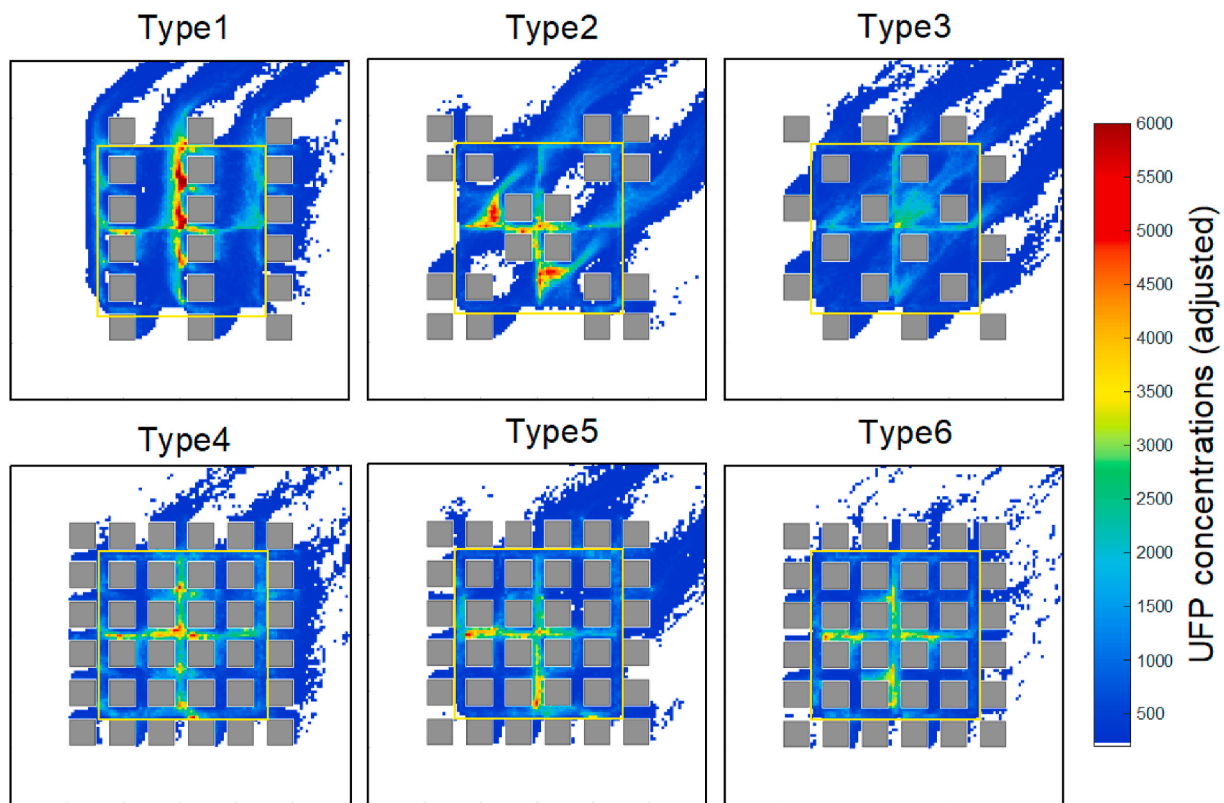


Fig. 5. Averaged UFP concentrations for six built environment types for different wind directions, south (S), southwest (SW), west (W), and northwest (NW). As the configurations are symmetric, directions rotated by 180° are not shown; Types 3 and 6 are not diagonally symmetric so NW is also shown for these layouts.

(Fig. 5), and winds coming from the southwest (hitting the corners of the buildings) produced the most varied results. We show the spatial distribution maps of the average UFP concentrations at street level (0.4–2 m AGL) for southwesterly winds in Fig. 6. The remaining wind directions are shown in the supplementary material (Figure S2). Taken together, the figures also show the high dependence of hotspot formation and location on wind direction.

For the same building volume density, UFP concentrations at street level are generally lower for the built environments that have taller buildings and more open space between buildings (Type 1–3 vs Type 4–6, Fig. 6). Further, UFP concentrations at street level were highest if the tall buildings were arranged in rows with deep street canyons between buildings, except when winds were parallel to the building rows (Type 1 vs Type 2–3; Type 4 vs Type 5–6, Fig. 6). This was followed by buildings arranged in clusters (Types 2 and 5). The configuration that consistently showed the lowest concentrations was type 3, the ‘checkerboard’, a configuration in which streets have adjacent buildings on only one side of the street.

Average differences between the idealized layouts (Fig. 5) were smaller than for the observations (Figs. 2 and 3). However the observations span much wider ranges of building densities; 15 vs. 1.5–42 for the simulations and observations respectively. All of the simulated configurations also have similar Ar_{area} values; 0.399 for Types 1–3, slightly higher than 0.304 for types 4–6. These Ar_{area} values fall on a part of the curve that is relatively flat (Fig. 2), although the Ar_{area} values alone should make concentrations for types 1–3 higher than 4–6, the opposite of what was observed. The Ar_{area} is an empirically derived relationship that weighs building height slightly more than the ground-



UFP concentrations at street levels. Wind direction: Southwest

Fig. 6. The averaged UFP concentrations at street level (from 0.4 m to 2 m above the ground) for all six types with wind coming from southwest. The yellow squares show the area within which ground level concentrations were averaged (outside areas only; not within buildings). (For interpretation of the references to color in this figure legend, the reader is referred to the Web version of this article.)

level open space. For sites with similar $A_{r_{area}}$ values, the open space appears to have larger importance.

In addition to wind direction, we also explored the effect of wind speed. We set up three different wind speeds, at 0.5 m s^{-1} , 1 m s^{-1} and 2 m s^{-1} and used a fixed wind direction (southwest). The spatial map is shown in Figure S4. The averaged UFP concentrations of all six types over the domain with these three different wind speeds are compared in Figure S5. As expected, the UFP concentrations decreased with increasing wind speed. The same trends in concentrations were observed

for all wind speeds, but the differences between layouts were largest for 0.5 m s^{-1} and smallest for 2 m s^{-1} .

4.2. Vertical pollutant profiles

The vertical distribution of traffic-related pollution near tall residential buildings is a concern for residents on upper floors, but observations of vertical profiles of pollutants on urban streets are limited and difficult to obtain (Morawska et al., 1999; Wu et al. 2002, 2013; Quang

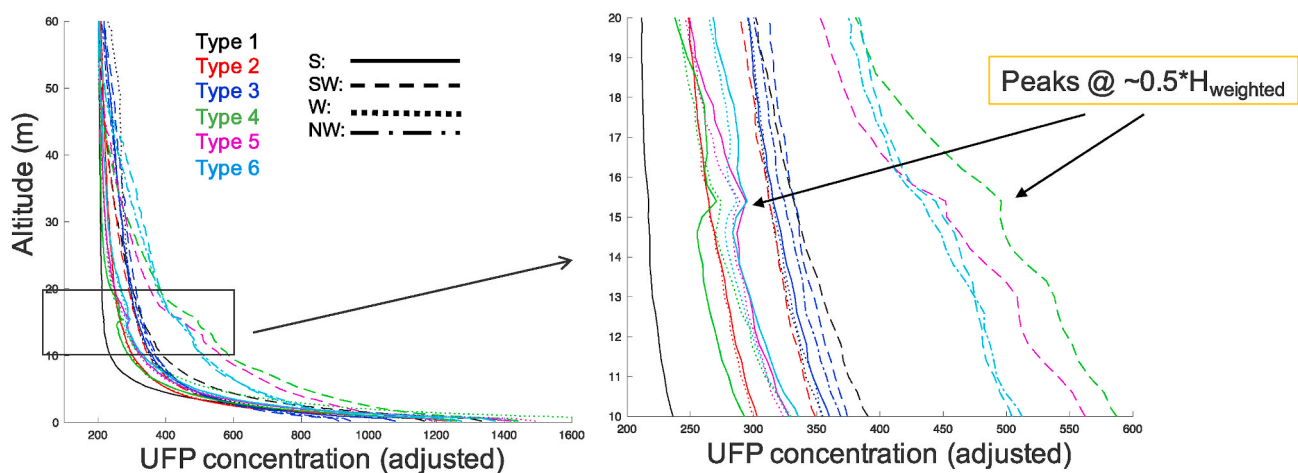


Fig. 7. Averaged profile of UFP concentrations over the main, sub-main streets and open space in the 2×2 city blocks. Line colors represent corresponding built types and different line styles represent simulation with different wind directions. Arrows point out the peaks. $H_{weighted}$ represents the mean area weighted building height for corresponding type. (For interpretation of the references to color in this figure legend, the reader is referred to the Web version of this article.)

et al., 2012). Spatially averaged vertical concentration profiles from QUIC simulations for the six idealized urban built environments are shown in Fig. 7 and the five sites in the Los Angeles area are shown in SI Figure S6. Generally, UFP concentrations decrease rapidly with increasing height for all configurations, especially within the first 10 m. For types 4–6 the UFP concentrations have one or more small peaks at around 15 m. 15 m was both half of the mean area weighted building height, H_{weighted} for type 4–6 and the roof height of the shorter buildings. The small elevated peaks may be due to the 15 m roof level of the shorter buildings as rooftops can trap pollutants in a rooftop recirculation (Bagal et al., 2004). This feature was also seen in the Los Angeles site configurations; Figure S6 shows that the Broadway & 7th site and Wilshire & Carondelet sites have additional concentration peaks at upper levels ($0.65 * H_{\text{weighted}}$) in some measurement sessions. The modeling results are in good agreement with observational results; Marini et al. (2014) measured UFP concentrations at seven street canyon sites in an Italian city between two canyon sides of an Italian city and found the peak occurs at non-surface level site ($0.38 * H_{\text{mean}}$) on the leeward side. Moreover, our model results also match the findings of Marini et al. (2014) that particle number concentrations decrease with increasing rooftop wind speed (Figure S4 and S5).

4.3. Model limitations: traffic-induced turbulence (TT), turbulent kinetic energy as a model output, and canopy effects

Although QUIC was able to reproduce the main relationship between representative built environment parameters (e.g., A_{area}), there are additional factors that should be considered in future developments. These include a parameterization for traffic induced turbulence, canopy effects, and an option to output turbulent kinetic energy (TKE) from the model. Turbulence that is very close to roads (traffic-induced turbulence, TT) differs strongly from that over natural surfaces (e.g., Rao et al., 1979; Kalthoff et al., 2005). Many computational and experimental studies have confirmed that turbulence induced by road traffic should not be neglected in the dispersion of trace gases in near roadway environments (Rao et al., 1979; Kalthoff et al., 2005; Alonso-Estébanez et al., 2012). Recently, more researchers have included the TT effects in atmospheric turbulence models, finding it improves the fit with field measurements (Katolický and Jícha 2005; Dong and Chan 2006; Xia et al., 2006).

In our study, we found that the simulated wind data for the sidewalks had lower spatial variability observed by Choi et al. (2016). Our hypothesis was that the observations were influenced by TT, which is not included in the QUIC model. This might be verifiable if TKE were available as an output from the QUIC model. Further, there is strong evidence from the observations that the surface level TKE increases sharply with building heterogeneity (Choi et al., 2016), and this has an indirect effect on the surface level pollution dispersion through turbulent processes, but the QUIC model performance cannot be probed in this regard.

In our study, we did not include vegetation because a comprehensive vegetation map was not available for the Los Angeles region. However, vegetative canopies, including trees and bushes are reasonably common along streets in the study area. Taking advantage of the vegetative canopy drag and turbulence scheme in QUIC could significantly impact the plume dispersion downwind and change the pollutant concentrations. Nelson et al. (2009) has shown that the canopy traps the plume and lowers wind velocities within and after the canopy, increasing exposure time in the canopy and downwind areas. In future studies, if vegetative canopy input data can be obtained, including these may also improve model performance (Nelson et al., 2009).

TT and vegetation have opposing effects on dispersion, however, so omitting both processes may have a muted effect, the sign of which is not known.

4.4. Recommendations for urban design

Our research findings suggest three features of the built environment can improve dispersion and lower concentrations in the built environment: 1) Placing more open space immediately adjacent to roadways; 2) Using taller buildings and more open space instead of shorter buildings and less open space; and 3) Avoiding arranging buildings in rows.

CRedit authorship contribution statement

Liye Zhu: Methodology, Investigation, Data curation, Writing - original draft, Writing - review & editing, Visualization. **Dilhara Ranasinghe:** Methodology, Resources, Data curation. **Marcelo Chamecki:** Methodology, Writing - review & editing. **Michael J. Brown:** Validation, Writing - review & editing. **Suzanne E. Paulson:** Conceptualization, Funding acquisition, Methodology, Project administration, Writing - original draft, Writing - review & editing.

Declaration of competing interest

The authors declare that they have no known competing financial interests or personal relationships that could have appeared to influence the work reported in this paper.

Acknowledgements

This project was supported by UCLA Institute of Transportation Studies, Los Angeles, California, USA, and made possible through funding received from the State of California via the Public Transportation Account grant number LA1701. We thank Prof. Wonsik Choi (Pusan National University, Busan, South Korea) for help with the UFP observational data. The contents of this report reflect the views of the authors, who are responsible for the facts and the accuracy of the information presented. This document is disseminated under the sponsorship of the State of California in the interest of information exchange and does not necessarily reflect the official views or policies of the State.

Supporting Information

The SI includes: Wind data for QUIC inputs, building heights, layouts and simulation domains and simulated UFP concentrations averaged at street levels for each type with wind coming from each direction and with different wind speeds from one direction.

Appendix A. Supplementary data

Supplementary data to this article can be found online at <https://doi.org/10.1016/j.atmosenv.2021.118267>.

References

- Al-Dabbous, A.N., Kumar, P., 2014. The influence of roadside vegetation barriers on airborne nanoparticles and pedestrians exposure under varying wind conditions. *Atmos. Environ.* 90, 113–124.
- Alonso-Estébanez, A., Pascual-Muñoz, P., Yagüe, C., Laina, R., Castro-Fresno, D., 2012. Field experimental study of traffic-induced turbulence on highways. *Atmos. Environ.* 61, 189–196.
- Bagal, N.L., Singh, B., Pardyjak, E.R., Brown, M.J., 2004. Implementation of rooftop recirculation parameterization into the QUIC fast response urban wind model. *Fifth Conference on the Urban Environment*. American Meteorological Society.
- Becerra, T.A., Wilhelm, M., Olsen, J., Cockburn, M., Ritz, B., 2013. Ambient air pollution and autism in Los Angeles county, California. *Environ. Health Perspect.* 121 (3), 380–386.
- Behrentz, E., Sabin, L.D., Winer, A.M., Fitz, D.R., Pankratz, D.V., Colome, S.D., Fruin, S. A., 2005. Relative importance of school bus-related microenvironments to children's pollutant exposure. *J. Air Waste Manag. Assoc.* 55 (10), 1418–1430.
- Boarnet, M.G., Houston, D., Edwards, R., Princevac, M., Ferguson, G., Pan, H.S., Bartolome, C., 2011. Fine particulate concentrations on sidewalks in five Southern California cities. *Atmos. Environ.* 45 (24), 4025–4033.

- Boogaard, H., Kos, G.P.A., Weijers, E.P., Janssen, N.A.H., Fischer, P.H., van der Zee, S.C., de Hartog, J.J., Hoek, G., 2011. Contrast in air pollution components between major streets and background locations: particulate matter mass, black carbon, elemental composition, nitrogen oxide and ultrafine particle number. *Atmos. Environ.* 45 (3), 650–658.
- Bowker, G.E., Baldauf, R., Isakov, V., Khlystov, A., Petersen, W., 2007. The effects of roadside structures on the transport and dispersion of ultrafine particles from highways. *Atmos. Environ.* 41 (37), 8128–8139.
- Brown, M.J., 2018. Quick Urban and Industrial Complex (QUIC) CBR Plume Modeling System: Validation-Study Document. L. A. N. Laboratory.
- Buonanno, G., Fuoco, F.C., Stabile, L., 2011. Influential parameters on particle exposure of pedestrians in urban microenvironments. *Atmos. Environ.* 45 (7), 1434–1443.
- Chen, R., Hu, B., Liu, Y., Xu, J., Yang, G., Xu, D., Chen, C., 2016. Beyond PM_{2.5}: the role of ultrafine particles on adverse health effects of air pollution. *Biochim. Biophys. Acta* 1860 (12), 2844–2855.
- Choi, W., Hu, S., He, M., Kozawa, K., Mara, S., Winer, A.M., Paulson, S.E., 2013. Neighborhood-scale air quality impacts of emissions from motor vehicles and aircraft. *Atmos. Environ.* 80, 310–321.
- Choi, W., Paulson, S.E., 2016. Closing the ultrafine particle number concentration budget at road-to-ambient scale: implications for particle dynamics. *Aerosol. Sci. Technol.* 50 (5), 448–461.
- Choi, W., Ranasinghe, D., Bunavage, K., DeShazo, J.R., Wu, L.S., Seguel, R., Winer, A.M., Paulson, S.E., 2016. The effects of the built environment, traffic patterns, and micrometeorology on street level ultrafine particle concentrations at a block scale: results from multiple urban sites. *Sci. Total Environ.* 553, 474–485.
- Choi, W., Ranasinghe, D., DeShazo, J.R., Kim, J.-J., Paulson, S.E., 2018. Where to locate transit stops: cross-intersection profiles of ultrafine particles and implications for pedestrian exposure. *Environ. Pollut.* 233, 235–245.
- Choi, W.S., He, M., Barbesant, V., Kozawa, K., Mara, S., Winer, A.M., Paulson, S.E., 2012. Prevalence of wide areas of air pollutant impact downwind of freeway during pre-sunrise at several locations in Southern California. *Atmos. Environ.* 62, 318–327.
- Dong, G., Chan, T.L., 2006. Large eddy simulation of flow structures and pollutant dispersion in the near-wake region of a light-duty diesel vehicle. *Atmos. Environ.* 40 (6), 1104–1116.
- Gowardhan, A.A., Pardyjak, E.R., Senocak, I., Brown, M.J., 2011. A CFD-based wind solver for an urban fast response transport and dispersion model. *Environ. Fluid Mech.* 11 (5), 439–464.
- Heusinkveld, H.J., Wahle, T., Campbell, A., Westerink, R.H.S., Tran, L., Johnston, H., Stone, V., Cassee, F.R., Schins, R.P.F., 2016. Neurodegenerative and neurological disorders by small inhaled particles. *Neurotoxicology* 56, 94–106.
- Hoek, G., Boogaard, H., Knol, A., De Hartog, J., Slottje, P., Ayres, J.G., Borm, P., Brunekreef, B., Donaldson, K., Forastiere, F., Holgate, S., Kreyling, W.G., Nemery, B., Pekkanen, J., Stone, V., Wichmann, H.E., Van der Sluijs, J., 2010. Concentration response functions for ultrafine particles and all-cause mortality and hospital admissions: results of a European expert panel elicitation. *Environ. Sci. Technol.* 44 (1), 476–482.
- Kalthoff, N., Baumer, D., Corsmeier, U., Kohler, M., Vogel, B., 2005. Vehicle-induced turbulence near a roadway. *Atmos. Environ.* 39, 5737–5749.
- Katolický, J., Jícha, M., 2005. Eulerian–Lagrangian model for traffic dynamics and its impact on operational ventilation of road tunnels. *J. Wind Eng. Ind. Aerod.* 93 (1), 61–77.
- Kheirbek, I., Haney, J., Douglas, S., Ito, K., Matte, T., 2016. The contribution of motor vehicle emissions to ambient fine particulate matter public health impacts in New York City: a health burden assessment. *Environ. Health* 15 (1), 89.
- LARIAC, 2009. Los Angeles Region Imagery Acquisition Consortium (LARIAC) Data Archives. Los Angeles, County GIS Data Portal.
- Lin, S., Munsie, J.P., Hwang, S.A., Fitzgerald, E., Cayo, M.R., 2002. Childhood asthma hospitalization and residential exposure to state route traffic. *Environ. Res.* 88 (2), 73–81.
- Manigrasso, M., Natale, C., Vitali, M., Protano, C., Avino, P., 2017. Pedestrians in traffic environments: ultrafine particle respiratory doses. *Int. J. Environ. Res. Publ. Health* 14 (3), 288–300.
- Marini, S., Buonanno, G., Stabile, L., Avino, P., 2014. A benchmark for numerical scheme validation of airborne particle exposure in street canyons. *Environ. Sci. Pollut. Res. Int.* 22.
- Morawska, L., Ristovski, Z., Jayaratne, E.R., Keogh, D.U., Ling, X., 2008. Ambient nano and ultrafine particles from motor vehicle emissions: characteristics, ambient processing and implications on human exposure. *Atmos. Environ.* 42 (35), 8113–8138.
- Morawska, L., Thomas, S., Gilbert, D., Greenaway, C., Rijnders, E., 1999. A study of the horizontal and vertical profile of submicrometer particles in relation to a busy road. *Atmos. Environ.* 33 (8), 1261–1274.
- Nelson, M., Williams, M., Zajic, D., Pardyjak, E., Brown, M., 2009. Evaluation of an Urban Vegetative Canopy Scheme and Impact on Plume Dispersion AMS 8th Symp. Urban Env., Phoenix, AZ.
- Patel, M.M., Chillrud, S.N., Correa, J.C., Feinberg, M., Hazi, Y., Deepti, K.C., Prakash, S., Ross, J.M., Levy, D., Kinney, P.L., 2009. Spatial and temporal variations in traffic-related particulate matter at New York City high schools. *Atmos. Environ.* 43 (32), 4975.
- Pearson, R.L., Wachtel, H., Ebi, K.L., 2000. Distance-weighted traffic density in proximity to a home is a risk factor for leukemia and other childhood cancers. *J. Air Waste Manag. Assoc.* 50 (2), 175–180.
- Pirjola, L., Lähde, T., Niemi, J.V., Kousa, A., Rönkkö, T., Karjalainen, P., Keskinen, J., Frey, A., Hillamo, R., 2012. Spatial and temporal characterization of traffic emissions in urban microenvironments with a mobile laboratory. *Atmos. Environ.* 63, 156–167.
- Quang, T.N., He, C., Morawska, L., Knibbs, L.D., Falk, M., 2012. Vertical particle concentration profiles around urban office buildings. *Atmos. Chem. Phys.* 12 (11), 5017–5030.
- Raaschou-Nielsen, O., Sorensen, M., Ketzel, M., Hertel, O., Loft, S., Tjønneland, A., Overvad, K., Andersen, Z.J., 2013. Long-term exposure to traffic-related air pollution and diabetes-associated mortality: a cohort study. *Diabetologia* 56 (1), 36–46.
- Ranasinghe, D., Lee, E.S., Zhu, Y., Frausto-Vicencio, I., Choi, W., Sun, W., Mara, S., Seibt, U., Paulson, S.E., 2018. Effectiveness of vegetation and sound wall-vegetation combination barriers on pollution dispersion from freeways under early morning conditions. *Sci. Total Environ.* (Press).
- Ranasinghe, D.R., Wonsik Choi, A. M. Winer, Paulson, S.E., 2016. Developing high spatial resolution concentration maps using mobile air quality measurements. *Aerosol and Air Quality Research* 16 (8), 1841–1853.
- Rao, S.T., Sedefian, L., Czapski, U.H., 1979. Characteristics of turbulence and dispersion of pollutants near major highways. *J. Appl. Mech.* 18 (3), 283–293.
- Riediker, M., Devlin, R.B., Griggs, T.R., Herbst, M.C., Bromberg, P.A., Williams, R.W., Cascio, W.E., 2004. Cardiovascular effects in patrol officers are associated with fine particulate matter from brake wear and engine emissions. *Part. Fibre Toxicol.* 1 (1), 2.
- Röckle, R., 1990. Bestimmung der Stömungsverhältnisse im Bereich komplexer Bauwerksstrukturen. . PhD Thesis, der Technischen Hochschule.
- Seinfeld, J.H., Pandis, S.N., 1998. *Atmospheric Chemistry and Physics*. Wiley, Hoboken, NJ, USA.
- Wu, C.-D., MacNaughton, P., Melly, S., Lane, K., Adamkiewicz, G., Durant, J.L., Brugge, D., Spengler, J.D., 2013. Mapping the vertical distribution of population and particulate air pollution in a near-highway urban neighborhood: implications for exposure assessment. *J. Expo. Sci. Environ. Epidemiol.* 24, 297.
- Wu, Y., Hao, J., Fu, L., Wang, Z., Tang, U., 2002. Vertical and horizontal profiles of airborne particulate matter near major roads in Macao, China. *Atmos. Environ.* 36 (31), 4907–4918.
- Xia, J.Y., Leung, D.Y.C., Hussaini, M.Y., 2006. Numerical simulations of flow-field interactions between moving and stationary objects in idealized street canyon settings. *J. Fluid Struct.* 22 (3), 315–326.